International Journal of
Molecular Sciences

Article

Ternary Cu(II) Complex with GHK Peptide and *Cis*-Urocanic Acid as a Potential Physiologically Functional Copper Chelate

Karolina Bossak-Ahmad [1], Marta D. Wiśniewska [1], Wojciech Bal [1], Simon C. Drew [1,2] and Tomasz Frączyk [1,*]

1 Institute of Biochemistry and Biophysics, Polish Academy of Sciences, Pawińskiego 5a, 02-106 Warsaw, Poland; karolina.bossak@gmail.com (K.B.-A.); marta.d.wisniewska@gmail.com (M.D.W.); wojciech.bal.ibb@gmail.com (W.B.); scdrew1@gmail.com (S.C.D.)

2 Department of Medicine (Royal Melbourne Hospital), The University of Melbourne, Melbourne 3010, Australia

* Correspondence: tfraczyk@ibb.waw.pl

Received: 21 July 2020; Accepted: 25 August 2020; Published: 27 August 2020

Abstract: The tripeptide NH_2–Gly–His–Lys–COOH (GHK), *cis*-urocanic acid (*cis*-UCA) and Cu(II) ions are physiological constituents of the human body and they co-occur (e.g., in the skin and the plasma). While GHK is known as Cu(II)-binding molecule, we found that urocanic acid also coordinates Cu(II) ions. Furthermore, both ligands create ternary Cu(II) complex being probably physiologically functional species. Regarding the natural concentrations of the studied molecules in some human tissues, together with the affinities reported here, we conclude that the ternary complex [GHK][Cu(II)][*cis*-urocanic acid] may be partly responsible for biological effects of GHK and urocanic acid described in the literature.

Keywords: copper; ternary complex; imidazole ligands

1. Introduction

The peptide Gly–His–Lys (GHK) is a native constituent of human blood [1]. It has numerous actions, including wound-healing [2], anti-inflammatory [3], and anti-anxiety [4] activities which may result from the interaction with unidentified receptors. Importantly, GHK modulates the expression of many genes [5]. It was proposed that almost all of the observed effects of the peptide are evoked by a GHK–copper(II) complex [6].

Urocanic acid (UCA) is a component of natural moisturizing factor (NMF) in the uppermost layer of the skin (stratum corneum) [7]. It is also found in blood [8] and neurons [9]. UCA is the product of histidine deamination by histidine ammonia–lyase (histidase). The formed *trans* isomer (*trans*-UCA) isomerises to *cis*-UCA upon exposure to ultraviolet radiation (Scheme 1) [10]. Both isomers accumulate in stratum corneum, reaching millimolar concentrations [11,12], and are present in plasma at micromolar concentrations [8]. Recently, it was found that UCA can cross the blood–brain barrier and be transported into neurons. Furthermore, histidase activity has also been found in neurons [9]. Importantly, there is a positive correlation between the content of histidine (the substrate for production of UCA) and wound healing [13,14]. UCA has many functions, including skin hydration maintenance, pH regulation, UV protection, and immunosuppression [10,15,16].

We have previously shown that UCA can bind Ni(II) ions [17]. Bearing in mind the similarity of Ni(II) and Cu(II) complex formation with many low molecular weight compounds, copper binding by UCA is conceivable.

Interestingly, GHK and UCA coexist in some human tissues and have common biological activities, such as influencing the immune and nervous systems. Because each can also bind metal ions, we hypothesised that biologically active forms of GHK and UCA may include a ternary complex with Cu(II) ions.

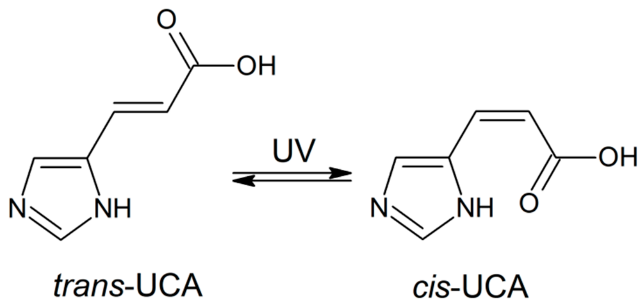

Scheme 1. UV-radiation-induced isomerisation of *trans*-urocanic acid (UCA) and *cis*-UCA [10].

In this work, we proved that GHK forms ternary Cu(II) complexes with *cis-/trans*-UCA. The results obtained by UV-vis and circular dichroism (CD) spectrophotometry, room-temperature electron paramagnetic resonance (EPR), and potentiometry suggest that such complexes can be present in the human body.

2. Results and Discussion

2.1. Interaction of Cu(II) with GHK

In order to thoroughly characterise the ternary interaction of urocanic acid, GHK, and Cu(II) we decided to revisit the Cu(GHK) coordination via spectroscopic and potentiometric studies. This step is necessary for precise comparison of experiments involving Cu/GHK and Cu/GHK/UCA. On that note, we also elaborated on $Cu(GHK)_2$, the complex that was reported previously by Conato et al. [18].

We report here a refined potentiometric model that incorporates *mono*- and *bis*- Cu(II) complexes with GHK and is supported by the spectroscopic characterization of these species. GHK has four exchangeable protons, attached (in the decreasing order of pK values) to the lysine side chain nitrogen, N-terminal amine, histidine imidazole (Im) nitrogen, and C-terminal carboxylate. Their protonation constants reported herein (Table S1) are in agreement with the literature data [19]. Potentiometry of Cu/GHK identified six Cu(II) species, namely $Cu(II)^{aq}$, CuH(GHK), Cu(GHK), CuH_{-1}(GHK), CuH_{-2}(GHK), and $CuH_2(GHK)_2$. The calculated logβ values and the ascribed protonation events are presented in Table S1. We validated our potentiometric model by combining two sets of pH-metric titrations with spectroscopic detection, the first set using 0.95 mM GHK in the presence of 0.8 mM $CuCl_2$ (Figure S1), and the second using a 20-fold molar excess of GHK (10.63 mM GHK and 0.5 mM $CuCl_2$). In an equimolar Cu/GHK solution, the variation in absorbance at 605 nm at low pH yielded a Hill coefficient of 2.03 ± 0.32, suggesting the cooperative formation of two species that can be ascribed to CuH(GHK) and Cu(GHK) stoichiometries. These 3N complexes differ only by the protonation state of the C-terminal carboxyl group and have identical *d–d* bands. Above pH 4.5, CD spectra obtained with a high excess of GHK exhibited a more prominent blue-shift compared with the equimolar complex. This suggests the coordination of an external nitrogen donor at the fourth planar Cu(II) site. Such complex corresponds to $CuH_2(GHK)_2$ stoichiometry. However, the observed changes in the electronic spectra are very similar to those seen previously in ternary complexes of other Xaa-His peptides (where Xaa is any amino acid residue except Pro) with imidazole (3+1N coordination, where three nitrogen atoms, $NH_3^{+\,(N\text{-}term)}$, N^{amide}, and N^{Im}, are from the first peptide molecule, and one nitrogen atom is N^{Im} from the second peptide molecule) [20,21]. Therefore, we assign the 3+1N coordination to this complex and propose to call it "auto-ternary", with the actual Cu(GHK)(H_2GHK) stoichiometry. Two additional deprotonations occur in the *mono*-complex at alkaline pH. The first probably corresponds to a water molecule (pK = 9.61) within the equatorial plane of the Cu(GHK) species [20,21]. Another is associated with the ε-amino nitrogen (pK = 10.77) from a side chain of Lys residue. The aforementioned assignment of the deprotonation to a water molecule instead of an imidazole N1 from another Cu(GHK) complex (with concomitant polynuclear species formation) is rationalized by the lack of drastic changes of CD parameters that would be expected upon formation of imidazole-bridged dimeric or tetrameric species [21–23].

The competitivity index (CI) [24,25] is a convenient parameter to compare the apparent affinities of complexes with various stoichiometries and protonation states. The value of CI equals to logβ of a complex MZ of a metal ion (M) with a theoretical ligand Z capable of outcompeting 50% of metal ion from the tested ligand or system of ligands at given conditions, such as specific pH and concentrations of reactants, when [Z] = [L] (L is a ligand to be compared). The Z molecule is supposed to bind only in 1:1 stoichiometry and to lack any deprotonating groups. This is equivalent to the assumption that $\sum_{ijkl}\left(\left[M_iH_jL_kA_l\right]\right) = [MZ]$. In simple cases, CI corresponds to conditional stability constant, ^{c}K. We used potentiometric data obtained for Cu/GHK and the CI method to calculate the conditional stability constants for the equimolar Cu(II)/GHK complex at [GHK] = [Cu] = 1 μM at pH 7.4, $^{c}K_{7.4}$ = 4.17 × 10^{12} M^{-1} and pH 6.5, $^{c}K_{6.5}$ = 4.79 × 10^{10} M^{-1}, corresponding to conditional dissociation constants of 0.24 and 20.9 pM, respectively. The CI value increases for higher excess of GHK over Cu(II), resulting from the formation of the auto-ternary $Cu(GHK)_2$ complex. However, the noticeable increase of CI was seen for millimolar concentrations of GHK (Figure S2).

Several groups have previously studied Cu/GHK complexes [18,26–28]. Our calculated protonation and formation constants values are closest to those obtained by Lau et al. [28] and Conato et al. [18], two groups that also utilised potentiometry to calculate the binding constants. Values published by others [26,27] (using EPR and ITC) are slightly higher than ours, most likely arising from the omission of $Cu(GHK)_2$ stoichiometry in their models.

As mentioned above, GHK coordinates copper via a tridentate nitrogenous chelate, with the fourth binding site, being open to coordination by an external ligand. This ligand can be a solvent molecule or, in the case of $Cu(GHK)_2$, an imidazole nitrogen of a second GHK molecule. To characterise the formation of this complex at physiological pH, we followed the titration of GHK into Cu(GHK) at pH 7.4 using UV-vis, EPR, and CD spectroscopies (Figure 1, Table S2), together with isothermal titration calorimetry (ITC, Figure S3, Table S3). Excess GHK caused a blue-shift of the absorbance maximum by 27 nm in the UV-vis spectra (Figure 1A) and by 28 nm in the CD spectra (Figure 1B). Room temperature EPR spectra revealed the presence of two motionally-averaged species delineated by clear isosbestic points (Figure 1C) confirming the existence of just two Cu(II) coordination modes. Simulations of the EPR spectra, including ligand hyperfine structure, were consistent with the assignment of 3N and 4N species for Cu(GHK) and $Cu(GHK)_2$, respectively (Figure S4, Table S2). Global fitting of all spectroscopic data yielded a value of $^{c}K_{7.4}$ = 237 ± 5 M^{-1} for the $Cu(GHK)_2$ complex (Figure 1D,E), while independent analysis of the ITC titrations yielded $^{c}K_{7.4}$ = 265 ± 46 M^{-1} (Figure S3). This value is significantly lower from the value ca. 500 M^{-1} that could be inferred from potentiometric stability constants reported by Conato et al. [18]. The retrospective analysis of experimental conditions in theirs, as well as our study indicates that such weak interactions could not be reliably determined by potentiometry, and our spectroscopic determination is the only valid approach.

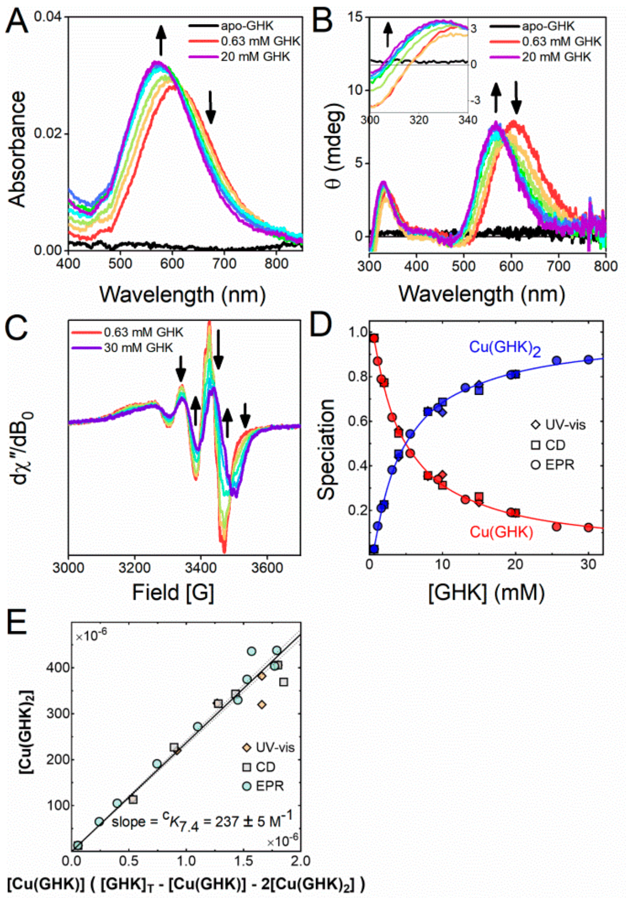

Figure 1. The conditional Cu(II) binding constant ${}^{c}K_{7.4}$ = [Cu(GHK)$_2$]/([Cu(GHK)][GHK]). (**A**) UV-vis, (**B**) circular dichroism (CD), and (**C**) electron paramagnetic resonance (EPR) spectra of Cu/GHK 0.5:n ($0.63 \leq n \leq 30$ mM) at pH 7.4, 25 °C. (**D**) Speciation diagram obtained by decomposition of all UV-vis (diamonds), CD (squares), and EPR (circles) spectra (Figures S4–S6). The solid lines were calculated using the binding constant derived from (**E**) and log ${}^{c}K_1$ = [Cu(GHK)]/([GHK][Cu]) = 12.62 derived from potentiometry. (**E**) Determination of the binding constant ${}^{c}K_{7.4}$ using least squares regression. The margin of error derives from the 95% confidence interval (dashed lines).

2.2. Interaction of Cu(II) with UCA

By analogy with the formation of Cu(GHK)$_2$, other external ligands could contribute to coordination sphere of Cu(GHK). Imidazole-based ligands can increase the overall affinity of metal complexes containing tridentate ligands by several orders of magnitude [20,29–33]. Urocanic acid, a by-product of L-histidine, contains an imidazole ring that could form a stable ternary Cu(II) complex with GHK in a manner similar to other Xaa-His peptides such as Trp–His–Trp–Ser–Lys–Asn–Arg, Gly–His–Thr–Asp, and Ala–His–His [20,21,34].

A series of control experiments was performed for both *cis*- and *trans*-UCA in presence of Cu(II). We have previously characterised the interaction of *cis*- and *trans*-UCA with Ni(II) ions and found out that the complexes were sufficiently stable to be of potential biological relevance [17]. Of the two isomers, *cis*-UCA binds Ni(II) ions more strongly owing to the chelate effect of its imidazole nitrogen and carboxyl oxygen. Thus, we focused on the binary and ternary Cu(II) complexes of *cis*-UCA and GHK. Logarithmic formation constants for Cu/*cis*-UCA complexes are provided in Table 1, and spectroscopic data used to validate the potentiometric model are shown in Figure 2.

Table 1. Protonation constants for *cis*-UCA (L) and logarithmic complex formation constants for the interaction of Cu(II) ions with *cis*-UCA, together with the ascribed protonation events.

Species	Logβ [1]	p*K*	Protonation Event
H_2L	9.541(6)	2.80	COOH
HL	6.742(2)	6.74	N^{Im}
CuL	4.941(9)		COOH, N^{Im}
CuL_2	8.76(1)		COOH, N^{Im}

[1] Values determined by potentiometry at 25 °C and I = 0.1 M (KNO_3). Standard deviations on the least significant digits, provided by HYPERQUAD [35] are given in parentheses.

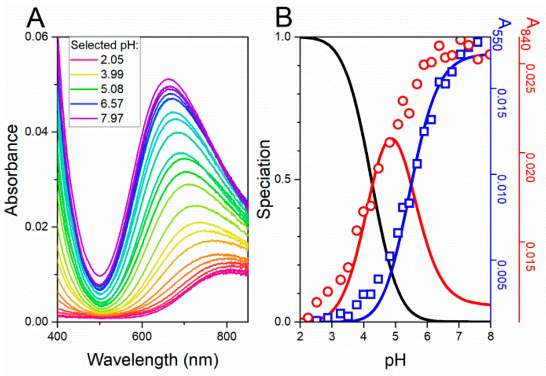

Figure 2. UV-vis spectra of 4 mM *cis*-UCA and 0.8 mM $CuCl_2$ titrated in a pH-metric manner. (**A**) Spectra are colour coded with reds (the lowest pH) to purples (the highest pH). (**B**) Species distribution of Cu(II) complexes of *cis*-UCA (red, Cu(*cis*-UCA); blue, Cu(*cis*-UCA)$_2$) at 25 °C, calculated for concentrations from UV-vis data (presented on panel A), based on protonation and stability constants shown in Table 1. Left-side axis represents molar fractions of Cu(II) complexes, right side axes stand for absorbance at 550 and 840 nm.

As expected based on the Irving–Williams series [36], the logβ value of Cu(*cis*-UCA) is higher than that of Ni(*cis*-UCA) (4.941 vs 3.406) [17]. Analogously, the formation constant of Cu(*cis*-UCA)$_2$ is higher than that of Ni(*cis*-UCA)$_2$ (8.76 vs. 6.239). Similar to the Ni(II) complex, the binding of the second *cis*-UCA molecule is weaker compared with the first (by 1.12 log units). This can be attributed to both a decreased number of bidentate binding modes for the second ligand and to the repulsion between the carboxyl groups of the two *cis*-UCA molecules. In the octahedral approximation of the complex structure, the first factor equals 0.38 (log(24/10)), resulting from lowering of the binding modes from 24 for the first molecule to 10 for the second one. Thus, the repulsion between carboxyl groups contributes stronger to weakening of the binding of the second *cis*-UCA molecule (0.74 log unit). The pH-dependent binding constant for the 1:1 Cu(*cis*-UCA) complex are ${}^{c}K_{7.4} = 7.16 \times 10^4$ M^{-1} and ${}^{c}K_{6.5} = 3.16 \times 10^4$ M^{-1}, respectively, corresponding to conditional dissociation constants 14.0 µM and 31.6 µM, respectively. However, as concentrations of *cis*-UCA are usually higher than the concentration of exchangeable Cu(II), the Cu(*cis*-UCA)$_2$ complex is promoted increasing the apparent affinity of this molecule to Cu^{2+} ions. Indeed, CI values for such complexes for 1 µM Cu(II) and millimolar *cis*-UCA levels are enhanced by at least one log unit (Figure S7). Lowering the pH slightly diminishes the strength of Cu(II) binding (by less than one log unit). The highest known concentrations of *cis*-UCA occur in the stratum corneum, and thus Cu(*cis*-UCA) complexes may occur mainly in the skin, however, a micromolar dissociation constant makes the Cu(*cis*-UCA) complex formation in blood plausible.

Cu(*trans*-UCA) was prone to precipitation under the same experimental conditions as Cu(*cis*-UCA), which prevented proper characterization of the binary complex. This precipitation may have resulted from lower stability of the Cu(*trans*-UCA) complex, leading to formation of insoluble $Cu(OH)_2$ at pH > 5. Indeed, control experiments confirmed that a molar excess of *trans*-UCA promoted the formation of a more stable CuL_2 complex.

2.3. Ternary Complex Formation of Cu/GHK/Imidazole

To quantify the ternary interaction of imidazole-based ligands with the Cu(GHK) complex at pH 7.4, we titrated up to 40 molar equivalents of Im into solutions containing 0.5 mM Cu(II) and 0.63 mM GHK and monitored the corresponding changes in the UV-vis, CD, and EPR spectra (Figure 3). Increasing concentrations of Im resulted in a blue-shift of the *d–d* transitions in the absorbance (35 nm), and CD (43 nm) spectra (Figure 3A,B). However, we did not observe any decrease in the overall ellipticity, indicating that a Cu(GHK)(Im) complex was formed rather than the achiral $Cu(Im)_n$ complexes (which are CD-silent). The isosbestic point at 601 nm (UV-vis) and the isodichroic point at 581 nm (CD) showed that Cu(GHK)(Im) was formed by the substitution of equatorial water in Cu(GHK) with Im. Room temperature EPR spectra revealed the presence of two motionally-averaged species delineated by clear isosbestic points (Figure 3C) confirming the existence of just two Cu(II) coordination modes, as in the Cu(GHK)/GHK experiment. Simulations of the EPR spectra, including ligand hyperfine structure, were consistent with the assignment of 3N and 4N species for Cu(GHK) and Cu(GHK)(Im), respectively (Figure S8, Table S2). The rotational correlation time of Cu(GHK)(Im) was comparable with that of Cu(GHK), as expected based upon their similar molecular weight. The magnetic parameters of Cu(GHK)(Im), however, were almost identical to those characterising $Cu(GHK)_2$, consistent with their common first coordination sphere. Further evidence for the proposed structure of the ternary species was obtained by substituting $^{15}N^{Im}$ with $^{14}N^{Im}$, which produced a change in the ligand hyperfine pattern expected for an equatorial Im ligand (Figure S8). Global fitting of all spectroscopic data yielded a value of $^{c}K_{7.4}$ = 725 ± 22 M^{-1} (Figure 3D,E) for Cu(GHK)(Im), which is comparable to the values previously reported for the Xaa-His peptides Trp–His–Trp–Ser–Lys–Asn–Arg (1022 ± 70 M^{-1}) and Gly–His–Thr–Asp (440 ± 14 M^{-1}) [20,21]. We also determined a value of $^{c}K_{7.4}$ = 532 ± 44 M^{-1} for Cu(GHK)(Im) complex using ITC (Figure S12 and Table S3). This is lower than the value obtained using spectroscopic methods, and it may stem from using HEPES buffer in ITC experiments.

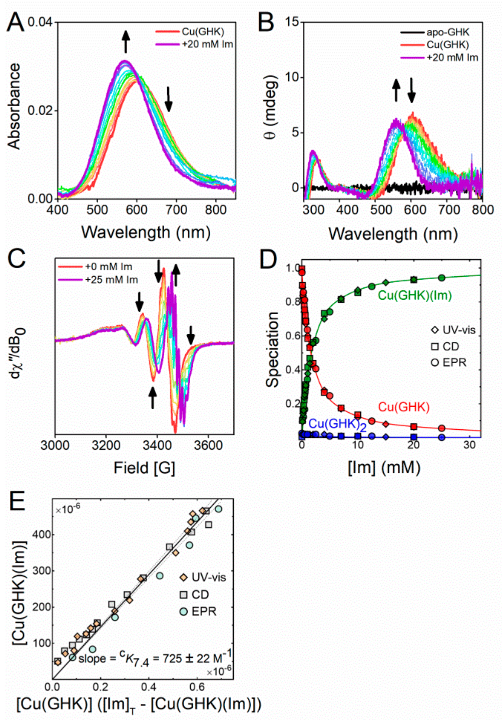

Figure 3. The conditional Cu(II) binding constant $^{c}K_{7.4}$ = [Cu(GHK)(Im)]/([Cu(GHK)][Im]). (**A**) UV-vis, (**B**) CD, and (**C**) EPR spectra of Cu/GHK/Im 0.5:0.63:*n* (0 ≤ n ≤ 25 mM) at pH 7.4, 25 °C. (**D**) Speciation of GHK complexes obtained from decomposition of UV-vis, CD, and EPR spectra in dependence of Im concentration (Figures S8–S11). (**E**) Determination of the binding constant $^{c}K_{7.4}$ using least squares regression. The margin of error derives from the 95% confidence interval (dashed lines).

Additionally, analysis of the ternary system was performed using CD and UV-vis pH-metric titrations of 0.95 mM GHK, 0.8 mM $CuCl_2$, and 50 mM Im, alongside a series of potentiometric titrations (Figure S13) in ratios of 1:0.9:4, 1:0.9:6, and 1:0.9:8 (GHK):(Cu):(Im). At pH below 5, five copper species were identified, namely an aqua ion (absorbance maximum at 816 nm), two imidazole copper complexes, Cu(Im) and $Cu(Im)_2$, and two 3N peptidic complexes, CuH(GHK) and Cu(GHK). Being achiral, the imidazole complexes are silent in CD spectra but produced a minor shoulder at 730 nm in UV-vis spectra at low pH. An increase of pH leads to the onset of Cu(GHK) dominance until an external imidazole begins to displace the complex's equatorial water ligand. This is visible by a 43 nm shift of the *d–d* band in CD spectra (Figure S13A,B). Under the given conditions (0.95 mM GHK, 0.8 mM $CuCl_2$, 50 mM Im, at pH 7.4), the ternary complex accounts for 96.5% of the available copper, while 3.4% and 0.2% are bound to Cu(GHK) and $Cu(GHK)_2$, respectively. Slightly less of the ternary complex (89.5%) is formed at pH 6.5, with Cu(GHK) accounting for 10.1% of available copper, the residual 0.4% being bound by $Cu(GHK)_2$ (Figure S13C).

2.4. Ternary Complex Formation of Cu/GHK/UCA

Knowing how imidazole interacts with Cu(GHK), we proceeded with the Cu(GHK) and UCA experiments. Due to the complexity of biological interactions and the possible translocation of UCA from stratum corneum to other locations that differ in pH, it is important to characterise the species distribution of the Cu/GHK/UCA system across a wide pH range. Because of the stronger interaction of Cu(GHK) with the *cis*-UCA isomer, and the aforementioned lower stability of Cu(*trans*-UCA), we focused on Cu/GHK/*cis*-UCA interactions.

First, we used potentiometry to characterise ternary Cu(GHK)(UCA) complex formation. We then validated the binding model using UV-vis and CD pH-metric titrations (Figure S14). Seven copper species were identified, namely the free copper aqua ion, Cu(*cis*-UCA), Cu(*cis*-UCA)$_2$ (minor), CuH(GHK), Cu(GHK), Cu(GHK)(*cis*-UCA) and a minor $CuH_2(GHK)_2$ species. The logβ value for the ternary Cu(GHK)(*cis*-UCA) is 19.29(2). At low pH (for 0.95 mM GHK, 0.8 mM Cu, and 6 mM *cis*-/*trans*-UCA), CD spectra of both Cu/GHK/*cis*-UCA and Cu/GHK/*trans*-UCA show *d–d* band at 606 nm, due to the prevalence of Cu(GHK) (Figure 4A,B). Simultaneously, a small proportion of binary urocanic acid complexes manifested as a reduced ellipticity compared with the Cu/GHK sample (Figure 4C,D). Both Cu(UCA) and $Cu(UCA)_2$ are CD silent, but noticeable in the absorbance spectra around 700 nm (Table S4, Figure S14, *cf* Figure 2). With increasing pH, the Cu(GHK) species begins to dominate but is quickly replaced above pH 4.9 by Cu(GHK)(UCA). Evidence for the latter species is provided by the blue-shift of *d–d* band corresponding to the 3N coordination sphere of Cu(GHK) (Figure 4A,B), and a comparison of the ellipticity of Cu/GHK and Cu/GHK/UCA samples at 650 nm (Figure 4C,D). The Cu(GHK)(UCA) complex is formed between pH 5–10 for both *cis*- and *trans*-UCA, as deduced from the reduced ellipticity at 650 nm in comparison with binary Cu(GHK). Although this description is qualitative, it can be estimated that *trans*-UCA forms less ternary complex than *cis*-UCA under the same experimental conditions, and thus it forms lower-stability ternary complex.

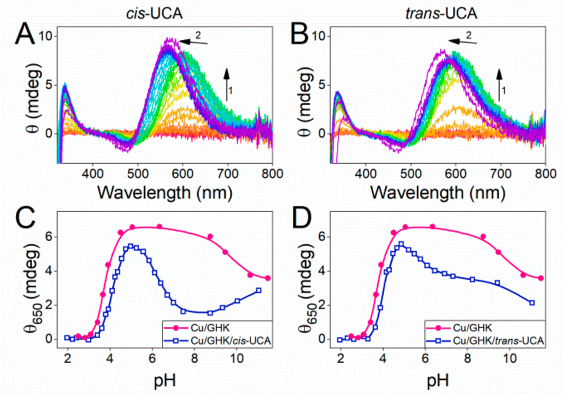

Figure 4. spectra of 0.95 mM GHK, 0.8 mM $CuCl_2$, and 6 mM *cis*-UCA (**A**) or *trans*-UCA (**B**) in pH-metric manner. Arrows indicate the spectral changes from low to high pH. The ellipticity at 650 nm was read from panels (A) and (B) and shown for *cis*-UCA (**C**) or *trans*-UCA (**D**) (navy squares) juxtaposed to data obtained via pH-metric titration of 0.95 mM GHK with 0.8 mM $CuCl_2$ (magenta circles).

In order to quantify the ternary complex formation for both *cis*- and *trans*-UCA, titrations of Cu/GHK with *cis*- and *trans*-UCA at pH 6.5 and 7.4 were performed to obtain conditional binding constants. Addition of UCA to solutions of Cu(GHK) at pH 6.5 and 7.4 created a blue-shift in both CD and UV-vis spectra (Figure 5 and Figures S15–S17) by ca. 46 nm for *cis*-UCA and 39 nm for *trans*-UCA suggesting coordination of an additional nitrogen ligand. Because Cu(II) and GHK were almost equimolar, the formation of $Cu(GHK)_2$ is limited and cannot be the cause of blue-shift. Sole competition between Cu(GHK) and Cu(UCA)/$Cu(UCA)_2$ at pH 6.5 and 7.4 can be also excluded since the achiral complexes of urocanic acid are CD-silent and thus competition would cause an overall decrease in the observed ellipticity of the Cu(GHK) complex. The concentration dependence of the ellipticity and absorbance changes with respect to the titrated ligands shows that *trans*-UCA did not reach equilibrium at the same concentration as *cis*-UCA, suggesting *trans*-UCA has a lower affinity for Cu(GHK) than *cis*-UCA. Indeed, the calculated conditional stability constants from a global fit of CD and UV-vis spectra of titrations with *cis*- and *trans*-UCA (Figure 5 and Figures S15–S17, Table 2) confirm this observation.

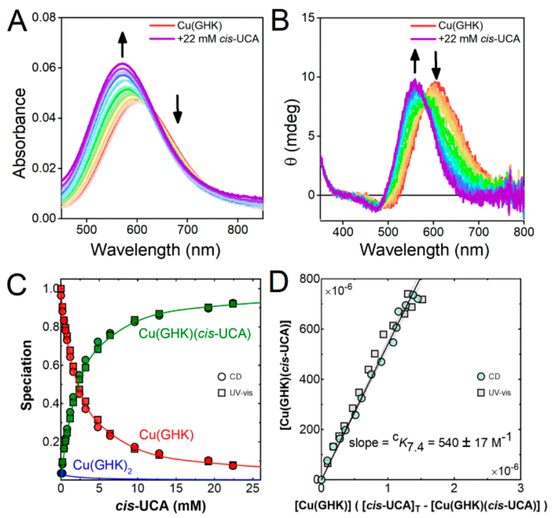

Figure 5. The conditional Cu(II) binding constant $^{c}K_{7.4}$ = [Cu(GHK)(*cis*-UCA)]/([Cu(GHK)][*cis*-UCA]). (**A**) UV-vis, and (**B**) CD spectra of Cu/GHK/*cis*-UCA 0.8:0.95:n ($0 \leq n \leq 22$ mM) at pH 7.4, 25 °C. (**C**) Speciation of GHK complexes obtained from decomposition of UV-vis and CD spectra in dependence of *cis*-UCA concentration. (**D**) Determination of the binding constant $^{c}K_{7.4}$ using least squares regression. The margin of error derives from the 95% confidence interval dashed lines).

Table 2. Binding constants of binary Cu(II) complexes of GHK, and ternary Cu(II) complexes of GHK with imidazole-bearing ligands at pH 6.5 and 7.4, at 25 °C.

Equilibrium	${}^{c}K_{6.5}$ (M^{-1})	${}^{c}K_{7.4}$ (M^{-1})
$Cu + GHK \rightleftarrows Cu(GHK)$	4.79×10^{10} [1]	4.17×10^{12} [1]
$Cu + cis^{-} - UCA \rightleftarrows Cu(cis - UCA)$	3.8×10^{4} [1]	7.94×10^{4} [1]
$Cu(GHK) + GHK \rightleftarrows Cu(GHK)_2$		237 ± 5 [2]
		265 ± 46 [3]
$Cu(GHK) + Im \rightleftarrows Cu(GHK)(Im)$		725 ± 22 [2]
		532 ± 44 [3]
$Cu(GHK) + cis^{-} - UCA \rightleftarrows Cu(GHK)(cis - UCA)$	345 ± 26 [4]	540 ± 17 [4]
$Cu(GHK) + trans^{-} - UCA \rightleftarrows Cu(GHK)(trans - UCA)$	186 ± 10 [4]	200 ± 10 [4]

The conditional binding constants were determined using: [1] potentiometric data; [2] UV-vis, CD, and EPR spectra; [3] ITC data; [4] UV-vis and CD spectra.

At pH 7.4, *cis*-UCA binds Cu(GHK) with ${}^{c}K_{7.4}$ 540 ± 17 M^{-1}, similar to imidazole, whereas the binding of *trans*-UCA is almost three times weaker with ${}^{c}K_{7.4}$ 200 ± 10 M^{-1}. This means that when both GHK and UCA are co-localised in the human body (e.g., in the blood), *cis*-UCA is favoured to form a ternary complex. Lowering the pH to 6.5 changes the situation, since the conditional binding constant for *trans*-UCA does not change (${}^{c}K_{6.5}$ = 186 ± 10 M^{-1}), but *cis*-UCA binding to Cu(GHK) is much reduced (${}^{c}K_{6.5}$ = 345 ± 26 M^{-1}). Thus, in the upper layers of the skin, where the pH is lower, formation of a ternary complex does not greatly favour *cis*-UCA over *trans*-UCA. The observed difference in pH sensitivity can be attributed to higher basicity of the imidazole moiety in *cis*-UCA than *trans*-UCA (pK_a values of 6.74 and 5.83, respectively) [17].

2.5. Biological Relevance

We chose pH values of 7.4 and 6.5 to represent the pH of the blood and the skin, respectively. UCA naturally occurs in the skin. GHK is probably released locally during collagen or SPARC (Secreted Protein Acidic and Rich in Cysteine) proteolysis caused by skin damage [37,38]. The pH at the surface of healthy skin is relatively low (ca. 5–6). However, there is a pH gradient (increasing up to 7.4) through all layers of the skin [39]. Importantly, the pH of the skin immediately increases after damage, being closer to 7.4 [39], and even above 8 [40,41]. Persistence of high pH is characteristic of a chronic wound [40,41]. Taking this into account, the known function of GHK as a healing factor may result from a stable ternary Cu(GHK)(*cis*-UCA) complex at pH 7–8. Binding of the ternary partner (*cis*-UCA) increases the apparent affinity of GHK for Cu(II) (Figure 6). Thus, the presence of such a complex after skin damage is plausible. The wound healing process involves several steps: haemostasis, inflammation, proliferation, and tissue remodeling [39]. The role of *cis*-UCA in immunosuppression has been revealed [10]. Therefore, it seems probable that this molecule, perhaps in the form of a ternary complex, prevents the inflammation step to develop into the chronic state. In this context, it is interesting that supplementation with histidine (a substrate for UCA synthesis) accelerates wound healing [14]. Furthermore, a deficiency in histidine was observed in skin wounds [13].

The formation of the ternary complex may also be of relevance to recent usage of UCA or Cu/GHK in cosmetics, anti-allergic or wound-healing-promoting materials, involving GHK immobilized on polymers or nanoparticles, or within liposomes [2,6,42–46].

Literature data regarding the concentrations of main components of natural moisturizing factor (NMF) in stratum corneum (43 mM serine, 30 mM glycine, 23 mM pyroglutamic acid, 18 mM alanine, 14 mM lactic acid, and 14 mM *cis*-UCA) [11,12] and Cu(II) complex formation constants [47,48] can be used to simulate the Cu(II) speciation. For this purpose, we calculated the molar fractions of Cu(II) species at pH 7.4 (representing the conditions found in wounds; Figure 7), and 6.5 (corresponding to healthy skin; Figure S18). We also assumed a GHK concentration of 0.6 μM, as found in human plasma. One can speculate that the local concentration of GHK may be even higher at the site of skin damage during wound healing. Furthermore, the application of wound-healing materials containing

GHK as the active substance can lead to an increase in the concentration of this peptide. Thus, we also calculated the Cu(II) speciation assuming 6 and 60 µM GHK. At pH 7.4 and the lowest concentration of GHK, the majority of Cu(II) is complexed with serine and glycine. However, 46% of copper bound to GHK is in the ternary Cu(GHK)(*cis*-UCA) complex. The latter percentage does not change for higher concentrations of GHK, but Cu(GHK)(*cis*-UCA), Cu(GHK)(carboxylates), (including carboxylic acids and amino acids binding monodentately via their carboxylic functions) [20], and Cu(GHK) start to dominate the overall Cu(II) speciation (Figure 7). Only slightly lower concentrations of Cu(GHK)(*cis*-UCA) and Cu(GHK) are predicted at pH 6.5 (Figure S18).

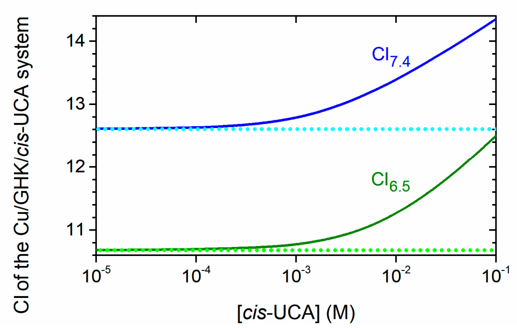

Figure 6. Influence of variable concentrations of *cis*-UCA on the apparent affinity of Cu/GHK/*cis*-UCA system. Values of $CI_{7.4}$ and $CI_{6.5}$ in the presence of *cis*-UCA (blue and green solid line) are valid for [Cu] = [GHK] = 1 µM, at pH 7.4 and 6.5, respectively. The dotted lines represent the reference $CI_{7.4}$ and $CI_{6.5}$ levels calculated for solutions without *cis*-UCA.

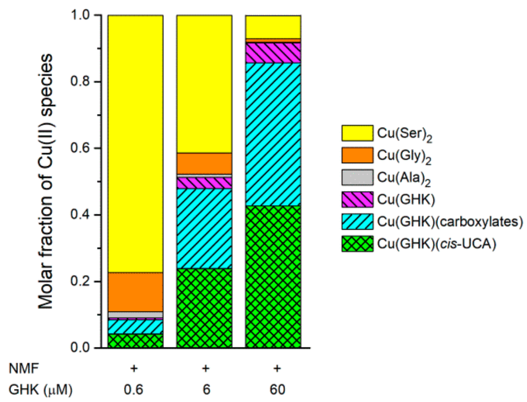

Figure 7. Species distribution simulated for natural moisturizing factor (NMF), 0.9 µM Cu^{2+} ions, and different concentrations of GHK, at pH 7.4 (representing the possible conditions in wounds). The lowest concentration of GHK (0.6 µM) is equal to the concentrations found in human plasma. Higher concentrations (6 and 60 µM) of GHK may occur in wounds and/or after application of cosmetics or other products with GHK as the active substance. The protonation constants and stability constants for Cu(II) complexes were taken from the literature [47,48] and this paper. The conditional constant for the ternary complexes formation of Cu(GHK) with carboxylates (68 M^{-1}) [20] was also included in calculations. Concentrations taken for calculations are 43 mM serine, 30 mM glycine, 23 mM pyroglutamic acid, 18 mM alanine, 14 mM lactic acid, and 14 mM *cis*-UCA [11,12]. All ternary complexes of Cu(GHK) with aforementioned compounds with carboxylic groups were combined in the "Cu(GHK)(carboxylates)". Only the species exceeding 1% of all Cu(II) species are shown for clarity.

GHK and UCA also are present in the blood, although at lower concentrations [8]. UCA crosses the blood–brain barrier and was even found in cerebrospinal fluid and neurons [9]. GHK was also found to be transported into the brain [6]. It remains of great interest to determine the relevance of the ternary Cu(GHK)(*cis*-UCA) complex to the neuronal environment.

Another important aspect of our findings is the ternary complex formation of Cu(GHK) with imidazole donors in general. The imidazole ring of the histidine residue in proteins and peptides can also form a ternary complex with an apparent affinity 1–2 orders of magnitude higher than Cu(GHK). Given the high abundance of His residues, the preferred Cu(II) complex of GHK will be ternary Cu(GHK)(N^{Im}) rather than binary Cu(GHK). A ternary complex has not been considered before, however, based on our data Cu(GHK) "attached" to bigger peptides or proteins may be the actual form available in blood. Indeed, one may speculate that the isolation of Cu(GHK) from a protein fraction of blood [49] is a consequence of ternary complex formation. A Cu(GHK)(N^{Im}) complex may also be the form relevant to other biological effects. For example, Miller et al. found that Cu(GHK) treatment inhibits lipid peroxidation when iron is sourced from ferritin [50]. Cu(GHK) complex was suggested to block physically the ferritin channel disabling the efflux of iron ions. We imply that formation of a ternary Cu(GHK)(N^{Im}) complex with one of the numerous His residues present at the channel opening is responsible for this action.

3. Materials and Methods

3.1. Materials

Gly-His-Lys (#G1887), Imidazole (#I5513), *cis*-UCA, *trans*-UCA, HCl, KNO_3, HNO_3, and $CuCl_2$ were purchased from Sigma-Aldrich (St. Louis, MO, USA). NaOH was obtained from Chempur (Piekary Slaskie, Poland). ^{65}CuO (>99%) was sourced from Cambridge Isotope Laboratories (Tewksbury, MA, USA). The 0.1 M NaOH solution for potentiometric titrations was purchased from POCH (Gliwice, Poland) and standardised via potentiometry using potassium hydrogen phthalate (Merck, Darmstadt, Germany).

3.2. UV-Vis & Circular Dichroism Spectroscopy

Spectroscopic measurements were carried out using a J-815 CD spectrometer (JASCO, Easton, MD, USA) and a Lambda 950 UV/vis/NIR spectrophotometer (PerkinElmer, Waltham, MA, USA) in the spectral ranges 270–800 and 270–850 nm, respectively. All experiments were performed at 25 °C in quartz cuvettes with a 1 cm path length.

3.2.1. pH-Metric Titrations

A series of titrations was recorded using UV-vis and CD spectroscopies. For understanding the Cu/GHK interaction we titrated (i) 0.95 mM GHK, 0.8 mM $CuCl_2$ and (ii) 10.63 mM GHK, 0.5 mM $CuCl_2$, ensuring an excess of GHK over copper ions. Additionally, 4.0 mM *cis-/trans*-UCA, 0.8 mM $CuCl_2$ was titrated with NaOH in pH ranges 2.05–9.19 and 2.01–5.89 for *cis-* and *trans*-UCA, respectively. At higher pH values, we observed precipitation of copper hydroxide. The final three sets of titrations aimed to understand ternary interaction between (i) 0.95 mM GHK, 0.8 mM $CuCl_2$ and 50 mM imidazole and (ii) 0.95 mM GHK, 0.8 mM $CuCl_2$, and 6 mM *cis-/trans*-UCA. All experiments were performed in the pH-range 2.5–11.5 (unless otherwise stated) with the pH adjusted by addition of minute amounts of NaOH.

3.2.2. Ligand Titrations

Ternary interactions were studied at two pH values, 6.5 and 7.4 by titrating Cu(GHK) with external ligands. A pH of 6.5 mimics the prevailing conditions in the upper layers of the skin, whereas pH 7.4 mimics the blood environment. Titration of imidazole into Cu(GHK) was done using 0.63 mM peptide, 0.5 mM $CuCl_2$, and up to 40 molar equivalents of imidazole. This titration was solely performed at pH 7.4 as a control experiment. Additionally, a titration of Cu(GHK) (0.95 mM peptide, 0.8 mM $CuCl_2$) with *cis-/trans*-UCA was carried out up to 20 molar equivalents of UCA.

3.3. EPR Spectroscopy

Samples were prepared at a Cu(II) concentration of 0.5 mM in water. A concentrated stock of $^{65}CuCl_2$ was made by dissolving ^{65}CuO in 36% *w/w* HCl, followed by removal of excess HCl under heat and addition of milliQ grade water (Millipore, Burlington, MA, USA). A separate sample was prepared for each point in the titration, with the pH measured using a microprobe (Metrohm, Herisau, Switzerland) and adjusted as required using concentrated NaOH. X-band (9.857 GHz) continuous-wave EPR spectra were obtained at room temperature (22 °C) using a Bruker Elexsys E500 spectrometer fitted with a Bruker super-high-Q probehead (ER 4122SHQE, Billerica, MA, USA) and a quartz flat cell (Wilmad, WG-808-Q) for sample containment. Equilibrium was allowed to be established, as ascertained by time-independence of the spectra. The following instrumental settings were used throughout: microwave power, 20 mW; magnetic field modulation amplitude, 5 G; field modulation frequency, 100 kHz; receiver time constant, 40.96 ms; receiver gain, 80 dB; sweep rate, 10 gauss s^{-1}; averages, 15. Baseline correction was performed by weighted subtraction of the spectrum obtained using a water blank. Spectral simulations were carried out as previously described [51].

EPR studies of Cu(II) complexes are frequently carried out at low temperatures because the spectra of frozen solutions are independent of the molecular weight. We initially characterised our ternary systems using this approach but found that the binding constant derived from analysis of the frozen solution spectra was almost two orders of magnitude higher than that obtained from the UV-vis and CD spectra. In contrast, room temperature EPR experiments presented herein yielded an excellent quantitative agreement with other spectroscopy. This apparent freezing artefact will be investigated and presented elsewhere.

3.4. Potentiometry

Potentiometric measurements were carried out using a 907 Titrando automatic titrator (Metrohm, Herisau, Switzerland), with a Biotrode combined glass electrode (Metrohm, Herisau, Switzerland). The electrode was calibrated daily via titration of 4 mM HNO_3/96 mM KNO_3 solution. A 100 mM NaOH solution (carbon dioxide free) was used as a titrant. The 1.5 mL samples were prepared in 4 mM HNO_3/96 mM KNO_3 solution. All titrations were performed under argon atmosphere at 25 °C, in the pH range from ca. 2.7 to 11.5. Three to five titrations were used for calculations of protonation constants and Cu(II) formation constants. The obtained data were processed using SUPERQUAD and HYPERQUAD 2008 programs [35,52].

3.4.1. GHK Preparation

Acetate counter-ions present in the commercial GHK preparations can hinder the analysis of potentiometric data. Prior to experiments, we therefore exchanged the acetate counter-ions with TFA via two cycles of peptide dilution in ca. 0.1% TFA, followed by freeze-drying.

3.4.2. Ligands

To calculate protonation constants and the concentration of the stock solution, we prepared samples with ca. (i) 1 mM GHK, (ii) 1–4 mM Im, and (iii) 1–4 mM *cis*-UCA. For each ligand, 3–4 samples were prepared in HNO_3/KNO_3.

3.4.3. Binary Complexes

Binary copper complex formation was studied for GHK and *cis*-UCA, respectively, using different molar ratios of $CuCl_2$ and ligands. For Cu/GHK, six samples were run in molar ratios of peptide to copper of 1:0.9 (n = 2), 1:0.5, 1:0.3 (n = 2) and 1:0.2, whereas for Cu/*cis*-UCA four molar ratios were studied: 3:0.8, 4:0.8, 5:0.8, and 8:0.8.

3.4.4. Ternary Complexes

The studied molar ratios of GHK/Cu/Im were: 1:0.9:4, 1:0.9:6 and 1:0.9:8. For each molar ratio two samples were prepared. For GHK/Cu/*cis*-UCA five samples were prepared in ratios of 1:0.9:4; 1:0.9:5; 1:0.9:6; 1:0.9:7; and 1:0.9:8.

3.5. Isothermal Titration Calorimetry

Calorimetric titrations were carried out on the Nano ITC Standard Volume calorimeter (TA Instruments, New Castle, DE, USA). The sample cell (950 μL) and syringe (250 μL) were filled with degassed buffered solutions (20 mM HEPES, 100 mM NaCl, pH 7.4) and titrations were performed by ten injections of volume 24 μL added at 1000 s intervals while stirring at 200 rpm, at 25 °C. Solution of 1:0.97 of GHK:$CuCl_2$ was titrated with Im or GHK in a range of 0.4 to 40 or 15 molar equivalents, respectively. The concentration of Im in the syringe was 12 mM. The concentrations of GHK in the syringe were 6 or 12 mM. The initial concentrations of GHK in the cell were 0.1, 0.25, 0.35, 0.5, and 1.0 mM, for Im titrations, and 0.25–0.5 mM, for GHK titrations. The obtained data were analyzed with the NanoAnalyze v. 3.11.0 software.

3.6. Binding Constant Calculations

Cu(GHK)$_2$. A self-consistent approach was used to isolate the EPR, UV-vis, and CD spectra of Cu(GHK) and Cu(GHK)$_2$ and determine ${}^cK_{7.4}$ for the equilibrium CuL + L ⇌ CuL_2, where L = GHK: (1) An initial guess was made for the value of ${}^cK_{7.4}$, which was used to calculate the theoretical speciation of CuL and CuL_2 at the minimum and maximum value of n in the titration Cu/GHK 1:n ($n_{min} \leq n \leq n_{max}$); (2) The above speciation provided weighting factors that were used to algebraically subtract the spectrum of Cu/L 1:n_{max} from that of Cu/L 1:n_{min}, and vice versa, thus isolating the spectra of CuL and CuL_2, respectively; (3) Linear combinations of these basis spectra were used to perform a least squares fit of the experimental spectra obtained at all intermediate stoichiometries n; (4) The obtained values of [CuL] and [CuL_2] were used to derive a value of ${}^cK_{7.4}$ from the gradient of a plot of [CuL_2] versus [CuL] × ($[Cu]_T$ − [CuL] − 2[CuL_2]), where $[Cu]_T$ is the total concentration of all forms of Cu(II). This experimental value of ${}^cK_{7.4}$ was then used as a new guess for ${}^cK_{7.4}$, and steps 1–4 were repeated iteratively until the experimental value of ${}^cK_{7.4}$ differed from the most recent guess by less than 1%. The above procedure was carried out separately for UV-vis, CD, and EPR data sets. These were then combined into a single plot of [CuL_2] versus [CuL] × ($[Cu]_T$ − [CuL] − 2[CuL_2]) and a global value of ${}^cK_{7.4}$ was determined using least squares nonlinear regression (without outlier removal) implemented in GraphPad Prism version 8.1.1 for Windows (GraphPad Software, San Diego, CA, USA, www.graphpad.com), and the error in ${}^cK_{7.4}$ was calculated from the 95% confidence interval derived from the regression analysis.

Cu(GHK)(Im), Cu(GHK)(trans-UCA), and Cu(GHK)(cis-UCA)

Using the known formation constants for Cu(GHK) and Cu(GHK)$_2$, and the previously isolated spectra of Cu(GHK) and Cu(GHK)$_2$, a self-consistent approach was used to isolate the spectrum of Cu(GHK)(Im), Cu(GHK)(*trans*-UCA), and Cu(*cis*-UCA) and determine the value of ${}^cK_{7.4}$ and/or ${}^cK_{6.5}$ for the equilibrium CuL + A ⇌ CuLA, where L = GHK and A = Im, *trans*-UCA, or *cis*-UCA: (1) An initial guess was made for the value of ${}^cK_{6.5}$ or ${}^cK_{7.4}$ and the theoretical speciation of CuL, CuL_2 and CuL was calculated for the minimum and maximum values of n in the titration Cu/L/A 1:1.25:n ($n_{min} \leq n \leq n_{max}$); (2) The above speciation provided weighting factors that were used to algebraically subtract the spectra of CuL and CuL_2 from the spectrum obtained for Cu/L/A 1:1.25:n_{max}, thus yielding the spectrum of CuLA; (3) Linear combinations of the CuL, CuL_2, and CuLA basis spectra were used to perform a least squares fit of the experimental spectra obtained at all intermediate stoichiometries n; (4) The obtained values of [CuL], [CuL_2] and [CuLA] were used to derive a value of ${}^cK_{6.5}$ or ${}^cK_{7.4}$ from the gradient of a plot of [CuLA] versus [CuL] × ($[A]_T$ − [CuLA]), where $[A]_T$ is the total concentration of all forms of Im, *trans*-UCA, or *cis*-UCA present in the sample. The experimental value of ${}^{c}K_{6.5}$ or ${}^{c}K_{7.4}$ was then used as a new guess for ${}^{c}K_{6.5}$ or ${}^{c}K_{7.4}$, and steps 1–4 were repeated iteratively until the experimental value of ${}^{c}K_{6.5}$ or ${}^{c}K_{7.4}$ differed from the most recent guess by less than 1%. The binding constants of $CuIm_n$ (n = 1–4), Cu(*trans*-UCA)$_n$ and Cu(*cis*-UCA)$_n$ (n = 1–2) were too low for these species to influence the results and were therefore not considered. The above procedure was carried out separately for UV-vis, CD, and EPR data sets. These were then combined into a single plot of [CuLA] versus [CuL] × ($[A]_T$ − [CuLA]), and a global value of ${}^{c}K_{6.5}$ or ${}^{c}K_{7.4}$ was determined using least squares nonlinear regression (without outlier removal) implemented in GraphPad Prism version 8.1.1 for Windows (GraphPad Software, San Diego, CA, USA, www.graphpad.com), and the error in ${}^{c}K_{6.5}$ or ${}^{c}K_{7.4}$ was calculated from the 95% confidence interval derived from the regression analysis.

4. Conclusions

Cu(II)-GHK is a tissue hormone serving as a wound healing factor. Urocanic acid, present as *cis* and *trans* isomers, is the abundant low molecular component of natural moisturizing factor (NMF) of the skin. We have demonstrated that both urocanic acid isomers, and in particular the stable *cis* isomer, form ternary complexes with Cu(GHK). The thorough quantitation of parent and ternary complexes provided the basis for numerical simulations of distribution of Cu(II) ions in NMF. These simulations indicated that Cu(GHK)(*cis*-UCA), but not the binary Cu(GHK) complex is a significant component of the copper pool in NMF. This result, and in general the formation of Cu(GHK)(Im), indicates an urgent need for investigations of biological properties of this and other ternary complexes of GHK.

Supplementary Materials: Supplementary materials can be found at http://www.mdpi.com/1422-0067/21/17/6190/s1.

Author Contributions: Conceptualization, K.B.-A., W.B., S.C.D., and T.F.; methodology, K.B.-A., W.B., S.C.D., and T.F.; formal analysis, K.B.-A., S.C.D., and T.F.; investigation, K.B.-A., M.D.W., and S.C.D.; writing—original draft preparation, K.B.A. and T.F.; writing—review and editing, K.B.-A., W.B., S.C.D., and T.F.; visualization, K.B.-A., S.C.D., and T.F.; supervision, W.B. and T.F.; project administration, T.F.; funding acquisition, W.B. and S.C.D. All authors have read and agreed to the published version of the manuscript.

Funding: This study was financed partly by National Science Center (Poland) Project 2016/23/B/ST5/02253. The equipment used was sponsored in part by the Centre for Preclinical Research and Technology (CePT), a project cosponsored by the European Regional Development Fund and Innovative Economy, The National Cohesion Strategy of Poland. S.C.D. was supported in part by a fellowship awarded from the Faculty of Medicine, Dentistry and Health Sciences, the University of Melbourne.

Conflicts of Interest: The authors declare no conflict of interest. The funders had no role in the design of the study; in the collection, analyses, or interpretation of data; in the writing of the manuscript, or in the decision to publish the results.

Abbreviations

GHK	Gly-His-Lys peptide
Im	imidazole
UCA	urocanic acid

References

1. Pickart, L.; Margolina, A. Regenerative and Protective Actions of the GHK-Cu Peptide in the Light of the New Gene Data. *Int. J. Mol. Sci.* **2018**, *19*, 1987. [CrossRef] [PubMed]
2. Wang, X.; Liu, B.; Xu, Q.; Sun, H.; Shi, M.; Wang, D.; Guo, M.; Yu, J.; Zhao, C.; Feng, B. GHK-Cu-liposomes accelerate scald wound healing in mice by promoting cell proliferation and angiogenesis. *Wound Repair Regen.* **2017**, *25*, 270–278. [CrossRef] [PubMed]
3. Park, J.R.; Lee, H.; Kim, S.I.; Yang, S.R. The tri-peptide GHK-Cu complex ameliorates lipopolysaccharide-induced acute lung injury in mice. *Oncotarget* **2016**, *7*, 58405–58417. [CrossRef] [PubMed]
4. Bobyntsev, I.I.; Chernysheva, O.I.; Dolgintsev, M.E.; Smakhtin, M.Y.; Belykh, A.E. Anxiolytic Effects of Gly-His-Lys Peptide and Its Analogs. *Bull. Exp. Biol. Med.* **2015**, *158*, 726–728. [CrossRef] [PubMed]

5. Pickart, L.; Vasquez-Soltero, J.M.; Margolina, A. GHK and DNA: Resetting the Human Genome to Health. *Biomed. Res. Int.* **2014**, *2014*, 1–10. [CrossRef] [PubMed]
6. Pickart, L.; Vasquez-Soltero, J.; Margolina, A. The Effect of the Human Peptide GHK on Gene Expression Relevant to Nervous System Function and Cognitive Decline. *Brain Sci.* **2017**, *7*, 20. [CrossRef]
7. Mohammad, T.; Morrison, H.; HogenEsch, H. Urocanic Acid Photochemistry and Photobiology. *Photochem. Photobiol.* **1999**, *69*, 115–135. [CrossRef]
8. Correale, J.; Farez, M.F. Modulation of multiple sclerosis by sunlight exposure: Role of cis-urocanic acid. *J. Neuroimmunol.* **2013**, *261*, 134–140. [CrossRef]
9. Zhu, H.; Wang, N.; Yao, L.; Chen, Q.; Zhang, R.; Qian, J.; Hou, Y.; Guo, W.; Fan, S.; Liu, S.; et al. Moderate UV Exposure Enhances Learning and Memory by Promoting a Novel Glutamate Biosynthetic Pathway in the Brain. *Cell* **2018**, *173*, 1716–1727. [CrossRef]
10. Gibbs, N.K.; Tye, J.; Norval, M. Recent advances in urocanic acid photochemistry, photobiology and photoimmunology. *Photochem. Photobiol. Sci.* **2008**, *7*, 655–667. [CrossRef]
11. Visscher, M.O.; Tolia, G.T.; Wickett, R.R.; Hoath, S.B. Effect of soaking and natural moisturizing factor on stratum corneum water-handling properties. *J. Cosmet. Sci.* **2003**, *54*, 289–300.
12. Rawlings, A.V.; Harding, C.R. Moisturization and skin barrier function. *Dermatol. Ther.* **2004**, *17*, 43–48. [CrossRef] [PubMed]
13. Dawson, B.; Favaloro, E.J. High Rate of Deficiency in the Amino Acids Tryptophan and Histidine in People with Wounds. *Adv. Skin Wound Care* **2009**, *22*, 79–82. [CrossRef] [PubMed]
14. Kim, Y.; Kim, E.; Kim, Y. l-histidine and l-carnosine accelerate wound healing via regulation of corticosterone and PI3K/Akt phosphorylation in d-galactose-induced aging models in vitro and in vivo. *J. Funct. Foods* **2019**, *58*, 227–237. [CrossRef]
15. Bruhs, A.; Eckhart, L.; Tschachler, E.; Schwarz, T.; Schwarz, A. Urocanic Acid: An Endogenous Regulator of Langerhans Cells. *J. Investig. Dermatol.* **2016**, *136*, 1735–1737. [CrossRef]
16. Krien, P.M.; Kermici, M. Evidence for the Existence of a Self-Regulated Enzymatic Process Within the Human Stratum Corneum—An Unexpected Role for Urocanic Acid. *J. Investig. Dermatol.* **2000**, *115*, 414–420. [CrossRef]
17. Wezynfeld, N.E.; Goch, W.; Bal, W.; Frączyk, T. Cis-Urocanic acid as a potential nickel binding molecule in the human skin. *Dalton Trans.* **2014**, *43*, 3196–3201. [CrossRef]
18. Conato, C.; Gavioli, R.; Guerrini, R.; Kozłowski, H.; Młynarz, P.; Pasti, C.; Pulidori, F.; Remelli, M. Copper complexes of glycyl-histidyl-lysine and two of its synthetic analogues: Chemical behaviour and biological activity. *Biochim. Biophys. Acta Gen. Subj.* **2001**, *1526*, 199–210. [CrossRef]
19. Burger, K. Biocoordination Chemistry. In *Equilibria in Biologically Active Systems*; Burger, K., Ed.; Ellis Horwood: Hemel Hempstead, UK, 1990; p. 349.
20. Bossak, K.; Mital, M.; Poznański, J.; Bonna, A.; Drew, S.; Bal, W. Interactions of α-Factor-1, a Yeast Pheromone, and Its Analogue with Copper(II) Ions and Low-Molecular-Weight Ligands Yield Very Stable Complexes. *Inorg. Chem.* **2016**, *55*, 7829–7831. [CrossRef]
21. Kotuniak, R.; Frączyk, T.; Skrobecki, P.; Płonka, D.; Bal, W. Gly-His-Thr-Asp-Amide, an Insulin-Activating Peptide from the Human Pancreas Is a Strong Cu(II) but a Weak Zn(II) Chelator. *Inorg. Chem.* **2018**, *57*, 15507–15516. [CrossRef]
22. Farkas, E.; Sóvágó, I.; Kiss, T.; Gergely, A. Studies on transition-metal–peptide complexes. Part 9. Copper(II) complexes of tripeptides containing histidine. *J. Chem. Soc. Dalton Trans.* **1984**, *3*, 611–614. [CrossRef]
23. Daniele, P.G.; Zerbinati, O.; Zelano, V.; Ostacoli, G. Thermodynamic and spectroscopic study of copper(II)-glycyl-L-histidylglycine complexes in aqueous solution. *J. Chem. Soc. Dalton Trans.* **1991**, 2711–2715. [CrossRef]
24. Krężel, A.; Wójcik, J.; Maciejczyk, M.; Bal, W. May GSH and l-His contribute to intracellular binding of zinc? Thermodynamic and solution structural study of a ternary complex. *Chem. Commun.* **2003**, *3*, 704–705. [CrossRef] [PubMed]
25. Jezowska-Bojczuk, M.; Kaczmarek, P.; Bal, W.; Kasprzak, K.S. Coordination mode and oxidation susceptibility of nickel(II) complexes with 2′-deoxyguanosine 5′-monophosphate and L-histidine. *J. Inorg. Biochem.* **2004**, *98*, 1770–1777. [CrossRef] [PubMed]

26. Trapaidze, A.; Hureau, C.; Bal, W.; Winterhalter, M.; Faller, P. Thermodynamic study of Cu^{2+} binding to the DAHK and GHK peptides by isothermal titration calorimetry (ITC) with the weaker competitor glycine. *J. Biol. Inorg. Chem.* **2012**, *17*, 37–47. [CrossRef] [PubMed]
27. Bruni, S.; Cariati, F.; Daniele, P.; Prenesti, E. Speciation and structure of copper(II) complexes with histidine-containing peptides in aqueous medium: A combined potentiometric and spectroscopic study. *Spectrochim. Acta Part A Mol. Biomol. Spectrosc.* **2000**, *56*, 815–827. [CrossRef]
28. Lau, S.J.; Sarkar, B. The interaction of copper(II) and glycyl-L-histidyl-L-lysine, a growth-modulating tripeptide from plasma. *Biochem. J.* **1981**, *199*, 649–656. [CrossRef]
29. Sundberg, R.J.; Martin, R.B. Interactions of histidine and other imidazole derivatives with transition metal ions in chemical and biological systems. *Chem. Rev.* **1974**, *74*, 471–517. [CrossRef]
30. Kenche, V.B.; Zawisza, I.; Masters, C.L.; Bal, W.; Barnham, K.J.; Drew, S.C. Mixed Ligand Cu^{2+} Complexes of a Model Therapeutic with Alzheimer's Amyloid-β Peptide and Monoamine Neurotransmitters. *Inorg. Chem.* **2013**, *52*, 4303–4318. [CrossRef]
31. Mital, M.; Zawisza, I.A.; Wiloch, M.Z.; Wawrzyniak, U.E.; Kenche, V.; Wróblewski, W.; Bal, W.; Drew, S.C. Copper Exchange and Redox Activity of a Prototypical 8-Hydroxyquinoline: Implications for Therapeutic Chelation. *Inorg. Chem.* **2016**, *55*, 7317–7319. [CrossRef]
32. Drew, S.C. The N Terminus of α-Synuclein Forms Cu^{II}-Bridged Oligomers. *Chem. A Eur. J.* **2015**, *21*, 7111–7118. [CrossRef] [PubMed]
33. Drew, S.C. Probing the quaternary structure of metal-bridged peptide oligomers. *J. Inorg. Biochem.* **2016**, *158*, 30–34. [CrossRef] [PubMed]
34. Gonzalez, P.; Bossak-Ahmad, K.; Vileno, B.; Wezynfeld, N.E.; El Khoury, Y.; Hellwig, P.; Hureau, C.; Bal, W.; Faller, P. Triggering Cu-coordination change in Cu(ii)-Ala-His-His by external ligands. *Chem. Commun.* **2019**, *55*, 8110–8113. [CrossRef] [PubMed]
35. Gans, P.; Sabatini, A.; Vacca, A. Investigation of equilibria in solution. Determination of equilibrium constants with the HYPERQUAD suite of programs. *Talanta* **1996**, *43*, 1739–1753. [CrossRef]
36. Irving, H.; Williams, R.J.P. The stability of transition-metal complexes. *J. Chem. Soc.* **1953**, 3192–3210. [CrossRef]
37. Lane, T.F.; Iruela-Arispe, M.L.; Johnson, R.S.; Sage, E.H. SPARC is a source of copper-binding peptides that stimulate angiogenesis. *J. Cell Biol.* **1994**, *125*, 929–943. [CrossRef]
38. Maquart, F.X.; Pickart, L.; Laurent, M.; Gillery, P.; Monboisse, J.C.; Borel, J.P. Stimulation of collagen synthesis in fibroblast cultures by the tripeptide-copper complex glycyl-L-histidyl-L-lysine-Cu^{2+}. *FEBS Lett.* **1988**, *238*, 343–346. [CrossRef]
39. Schreml, S.; Szeimies, R.M.; Karrer, S.; Heinlin, J.; Landthaler, M.; Babilas, P. The impact of the pH value on skin integrity and cutaneous wound healing. *J. Eur. Acad. Dermatol. Venereol.* **2010**, *24*, 373–378. [CrossRef]
40. Sharpe, J.R.; Booth, S.; Jubin, K.; Jordan, N.R.; Lawrence-Watt, D.J.; Dheansa, B.S. Progression of wound pH during the course of healing in burns. *J. Burn Care Res.* **2013**, *34*, 201–208. [CrossRef]
41. Ono, S.; Imai, R.; Ida, Y.; Shibata, D.; Komiya, T.; Matsumura, H. Increased wound pH as an indicator of local wound infection in second degree burns. *Burns* **2015**, *41*, 820–824. [CrossRef]
42. Peltonen, J.; Pylkkänen, L.; Jansén, C.; Volanen, I.; Lehtinen, T.; Laihia, J.; Leino, L. Three Randomised Phase I/IIa Trials of 5% Cis-urocanic Acid Emulsion Cream in Healthy Adult Subjects and in Patients with Atopic Dermatitis. *Acta Derm. Venereol.* **2014**, *94*, 415–420. [CrossRef] [PubMed]
43. Sharma, S.; Anwar, M.F.; Dinda, A.; Singhal, M.; Malik, A. In Vitro and in Vivo Studies of pH-Sensitive GHK-Cu-Incorporated Polyaspartic and Polyacrylic Acid Superabsorbent Polymer. *ACS Omega* **2019**, *4*, 20118–20128. [CrossRef] [PubMed]
44. Sun, L.; Li, A.; Hu, Y.; Li, Y.; Shang, L.; Zhang, L. Self-Assembled Fluorescent and Antibacterial GHK-Cu Nanoparticles for Wound Healing Applications. *Part. Part. Syst. Charact.* **2019**, *36*, 1–6. [CrossRef]
45. Jauhonen, H.M.; Laihia, J.; Oksala, O.; Viiri, J.; Sironen, R.; Alajuuma, P.; Kaarniranta, K.; Leino, L. Topical cis-urocanic acid prevents ocular surface irritation in both IgE -independent and -mediated rat model. *Graefe's Arch. Clin. Exp. Ophthalmol.* **2017**, *255*, 2357–2362. [CrossRef] [PubMed]
46. Mulder, G.; Patt, L.; Sanders, L.; Rosenstock, J.; Altman, M.; Hanley, M.; Duncan, G. Enhanced healing of ulcers in patients with diabetes by topical treatment with glycyl-L-histidyl-L-lysine copper. *Wound Repair Regen.* **1994**, *2*, 259–269. [CrossRef]

47. Yamada, Y.; Nakasuka, N.; Tanaka, M. Complexation of thyrotropin-releasing hormone and its related compounds with copper(II) and nickel(II) ions. *Inorg. Chim. Acta* **1991**, *185*, 49–56. [CrossRef]
48. Smith, R.M.; Martell, A.E. *Critical Stability Constants*; Plenum Press: New York, NY, USA, 1982; Volume 5, ISBN 9781461567639.
49. Pickart, L.; Thaler, M.M. Tripeptide in human serum which prolongs survival of normal liver cells and stimulates growth in neoplastic liver. *Nat. New Biol.* **1973**, *243*, 85–87.
50. Miller, D.M.; DeSilva, D.; Pickart, L.; Aust, S.D. Effects of glycyl-histidyl-lysyl chelated Cu(II) on ferritin dependent lipid peroxidation. *Adv. Exp. Med. Biol.* **1990**, *264*, 79–84. [CrossRef]
51. Bossak-Ahmad, K.; Frączyk, T.; Bal, W.; Drew, S.C. The Sub-picomolar Cu^{2+} Dissociation Constant of Human Serum Albumin. *ChemBioChem* **2020**, *21*, 331–334. [CrossRef]
52. Gans, P.; Sabatini, A.; Vacca, A. SUPERQUAD: An improved general program for computation of formation constants from potentiometric data. *J. Chem. Soc. Dalton Trans.* **1985**, 1195–1200. [CrossRef]